Geophys. J. Int. (2000) **141,** 639–646

Magnetostratigraphic reinvestigation of the Palaeocene/Eocene boundary interval in Hole 690B, Maud Rise, Antarctica

Jason R. Ali,[1] Dennis V. Kent[2] and Ernie A. Hailwood[3]

[1] *Department of Earth Sciences, University of Hong Kong, Pokfulam Rd, Hong Kong, China. E-mail: jrali@hkucc.hku.hk*
[2] *Lamont-Doherty Earth Observatory, Palisades,* NY10964, *USA and Department of Geological Sciences, Rutgers University, Piscataway,* NJ08854, *USA*
[3] *Core Magnetics, Frostrow Lane, Sedbergh, Cumbria,* LA10 5JS, *UK*

Accepted 2000 January 4. Received 1999 December 20; in original form 1998 June 4

SUMMARY

Hole 690B, drilled on Maud Rise near Antarctica, provides one of the most important Palaeocene/Eocene boundary interval sections. Magnetostratigraphy plays a key role in dating Palaeocene/Eocene boundary events, but there are two problems with the published scheme in Hole 690B. The first concerns major mismatches of several magnetozones and biozones in the succession. The second is an unexplained pervasive declination cluster, which should not be present in these azimuthally unoriented piston cores. To resolve these issues, a palaeomagnetic reinvestigation was carried out on 98 specimens from 12 cores through the upper Palaeocene–middle Eocene section in Hole 690B.

The bulk of the samples carry an approximately uniformly directed magnetically hard component resulting in a declination cluster effectively identical to that of the earlier study. The spurious magnetization can be explained either as an 'inward-radial magnetization' or as a 'core-split overprint'. By estimating the extent of the overprint within each sample, it has been possible to construct a filtered magnetostratigraphy for the section. The result is that many of the magnetozone–biozone mismatches are eliminated, and the record of the 2.5 Myr Chron C24r, which brackets the various events associated with the Palaeocene/Eocene boundary, is considerably cleaner. It is not possible to define the upper and lower boundaries of this magnetochron, so we recommend that the dating of the events within this section be based on the biostratigraphy only.

Key words: magnetization, magnetostratigraphy, marine sediments, Ocean Drilling Program.

INTRODUCTION

Hole 690B (65.16°S, 1.20°E) was drilled on the Maud Rise, off Antarctica (Fig. 1), during ODP Leg 113. Presumably because of the thin Oligocene–Neogene sediment pile and the physical properties of the pelagic lithologies, advanced piston coring recovered ~100 per cent of a 130 m thick upper Palaeocene–Eocene sequence at this hole. Following Kennett & Stott (1991), the oxygen and carbon isotope records (Stott *et al.* 1990) and benthic foraminiferal extinction (Thomas 1990) in this section have achieved global importance for studies of the Palaeocene/Eocene boundary interval. A dramatic δC^{13} excursion is now recognized not only in numerous marine sites (e.g. Zachos *et al.* 1992, 1994) but also in terrestrial sections (Koch *et al.* 1995; Stott *et al.* 1996). Thus, if the C isotope event is itself not selected as the soon-to-be-chosen Palaeocene/

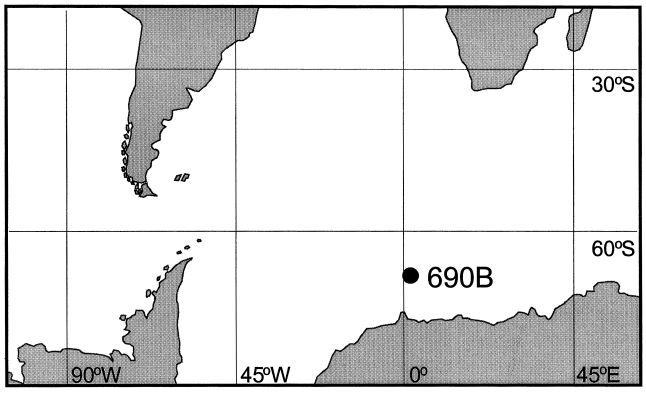

Figure 1. Map showing the location of Hole 690B on Maud Rise, near Antarctica.

Eocene boundary marker, then it will at least provide a key approximation of the boundary in sequences deposited in a wide variety of environments.

JUSTIFICATION FOR THE MAGNETOSTRATIGRAPHIC REINVESTIGATION

In order to date the isotope excursions and benthic foraminiferal extinction event in Hole 690B, various workers (Stott & Kennett 1990; Thomas 1990; Kennett & Stott 1991; Aubry *et al.* 1996; Thomas & Shackleton 1996) have drawn upon the calcareous nannofossil stratigraphy (Pospichal & Wise 1990) and magnetostratigraphy (Spiess 1990) to provide the chronostratigraphic ties for this hole. The other fossil groups, for example, the planktonic foraminifers (Stott & Kennett 1990), play only a limited role in constraining the Hole 690B events.

The reliability of the Hole 690B upper Palaeocene–lower Eocene magnetostratigraphic record has been questioned. Aubry *et al.* (1996) highlighted a $\sim$10 m thick dominantly normal-polarity magnetozone, which straddles the NP9/10 boundary (mid Chron C24r), that has no equivalent in the magnetobiostratigraphic scale (e.g. Berggren *et al.* 1995). A second critical magneto–biozone mismatch arises from the apparent record of Chron C25n, which in the published section extends well down into NP7, making the start of the chron about 1 Myr older than in the timescale of Berggren *et al.* (1995). Furthermore, Ali & Hailwood (1998) pointed out an unexplained consistent declination cluster (see Fig. 2) in the Hole 690B upper Palaeocene–middle Eocene piston cores (as well as most of the other piston cores in the hole). To clarify these concerns, a palaeomagnetic reinvestigation was carried out on the upper Palaeocene to lower middle Eocene (equivalent in part to nannofossil zones NP6–NP14) section in Hole 690B.

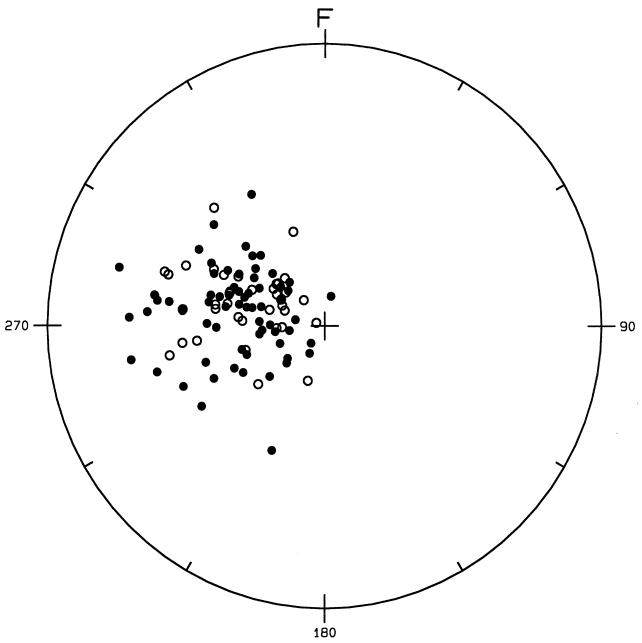

Figure 2. Stereographic plot showing the 270° declination cluster in Spiess's (1990, Appendix B) data set for specimens from Sections 14H-5 to 25H-6 at $\sim$25 cm and $\sim$100 cm below the top of each core section. Open/closed circles represent ChRM directions pointing up/down, respectively. F is an arbitrary azimuth. Note that Spiess sampled the entire 690B suite of sections at $\sim$25 cm intervals.

SAMPLING PROCEDURES

The Hole 690B cores were sampled by JRA at the ODP core repository at the Lamont-Doherty Earth Observatory, New York, in July 1997. Supplemented by the core descriptions, logs and photographs in the Leg 113 initial reports volume, and the information presented in Spiess (1990, Appendix B), an undisturbed piece of the core was selected and a 'way up' arrow was marked onto the surface of the split working half. A 4 to 6 cm long core piece was then removed from the core liner. A single specimen was cut from the piece and trimmed using a stainless steel knife or scalpel to fit snugly inside a 7.4 cm^3 cubic palaeomagnetic box (not the standard 6.0 cm^3 ODP issue). In most instances, there was no evidence of side-wall smearing of the sample against the inside of the palaeomagnetic box, indicating that there had been negligible disturbance to the sediment fabric. By sampling the cores in this way, it was hoped that 'push effect' overprint magnetizations (e.g. Lovlie *et al.* 1986; Hailwood *et al.* 1989; Hailwood & Clement 1991) would be avoided. The boxes were sealed using non-magnetic tape to minimize H_2O transfer to/from the sediment. In most cases, one or two samples were collected per 1.5 m length of core section, resulting in a total of 98 specimens from the upper Palaeocene to middle Eocene interval (Cores 14H–25H, which span 125.53–213.13 mbsf).

LABORATORY PROCEDURES

The palaeomagnetism laboratory work was carried out by JRA in the Southampton Oceanography Centre laboratory. Samples were measured using a 2G cryogenic magnetometer with an in-line stationary alternating field (AF) demagnetizer at 2.5 mT steps initially to 17.5 mT. Demagnetization above 17.5 mT was carried out using a Molspin AF tumbling demagnetizer in two-cycle reverse-rotate mode to minimize the potential effect of rotational remanent magnetizations. The samples were then measured using the 2G magnetometer. Demagnetization proceeded generally at 2.5 mT steps, mainly to 40 mT but occasionally to higher fields.

Demagnetization data were analysed using a Core Magnetics software package, which allows characteristic magnetization directions to be calculated using either Fisher (1953) statistics or principal component analyses (PCA, Kirschvink 1980). In practically all cases, the sample demagnetizations revealed stable magnetization (ChRM) components, and characteristic directions calculated using Fisher statistics had α_{95} values of $<4^\circ$ or PCA-method maximum angular dispersion values of $<5^\circ$. Examples of demagnetization behaviour are shown in Fig. 3. Remanence data are listed in Table 1.

RESULTS AND OBSERVATIONS

The reference frames used in the discussions below are illustrated in Fig. 4. A stereographic plot (Fig. 5), of the ChRM data from the 98 specimens indicates that the section carries an overprint magnetization. All but five of the specimens have ChRMs that point out of the core face with a clear cluster

Table 1. Summary of palaeomagnetic data from Hole 690B. mbsf: depth in metres below sea floor to the top of the specimen; Int: initial magnetic intensity in mA m^{-1}; Mx F: maximum applied demagnetizing field (in mT), which is 40 mT unless indicated; Md F (in mT): median destructive field (values preceded with an asterisk indicate the specimen carries a significant viscous magnetization); ChRM Dec/Inc directions are in coordinates from which the magnetostratigraphy is constructed; P: polarity with N normal, R reverse, ? indeterminate (absolute inclinations $<10^{\circ}$).

Spec.	Depth mbsf	Int	Mx F	Md F	Dec	Inc	P	Spec.	Depth mbsf	Int	Mx F	Md F	Dec	Inc	P
14H-5-103	125.53	1.883		27	124.6	66.7	R	19H-2-83	169.23	0.446	50	NR	69.4	53.4	R
14H-6-106	127.06	0.414		*27	139.3	67.2	R	19H-2-141	169.81	3.240		*4	122.6	56.2	R
14H-7-45	127.95	1.789		*32	123.0	82.0	R	19H-6-120	171.11	2.799		12	59.0	−48.4	N
15H-1-45	128.55	5.200		4	218.0	−38.3	N	19H3-139	171.30	8.806		9	92.6	55.3	R
15H-1-91	129.01	2.435		7	206.3	−27.1	N	19H-4-62	172.05	1.878		24	86.4	46.5	R
15H-2-15	129.75	2.757		7	175.2	29.5	R	19H-5-13	173.06	5.387		18	165.7	68.8	R
15H-2-88	130.48	4.325		7	156.1	21.2	R	20H-1-12	174.42	4.599		7	182.2	37.0	R
15H-2-140	131.00	7.854		4	173.6	29.5	R	20H-1-138	175.68	4.978		27	132.3	67.7	R
15H-3-46	131.56	2.772		7	137.5	−2.4	?	20H-2-84	176.64	8.351		22	149.4	71.9	R
15H-3-93	132.03	4.482		11	180.0	23.1	R	20H-2-142	177.22	7.110		25	136.0	63.6	R
15H-3-136	132.46	5.012		7	183.0	−5.5	?	20H-3-44	177.74	4.449		*31	132.6	74.2	R
15H-4-29	132.89	2.488		10	173.9	−21.0	N	20H-3-126	178.56	4.846		*6	127.9	67.9	R
15H-4-75	133.35	2.271		32	158.1	59.9	R	20H-4-85	179.65	7.658		24	168.4	73.5	R
15H4-141	134.01	2.866		9	166.1	55.6	R	21H-1-6	180.36	6.684		17	151.2	68.5	R
15H-5-20	135.30	3.626		25	149.4	59.0	R	21H-2-62	182.42	8.430		22	192.2	66.8	R
15H-6-43	136.03	5.225	60	33	171.0	66.5	R	21H-3-45	183.75	5.495	37.5	17	214.7	61.2	R
15H-6-127	136.87	5.381		12	178.6	12.1	R	22H-1-86	186.06	3.259		26	191.2	34.4	R
15H-7-5	137.15	4.115		13	170.7	21.9	R	22H-1-137	186.57	4.942	10	6	173.5	−41.0	N
15H-7-44	137.54	4.162		10	157.6	−59.9	N	22H-2-137	188.07	5.095		24	183.7	−59.3	N
16H-1-55	138.35	3.112		7	188.0	64.5	R	22H-3-54	188.74	5.086		8	171.7	−54.2	N
16H-1-127	139.07	8.323	60	20	252.4	−73.4	N	22H-4-68	190.38	5.043		33	206.5	−62.0	N
16H-2-66	139.96	1.086		22	223.5	59.3	R	22H-CC-1	190.96	6.789		21	204.7	−59.6	N
16H-2-137	140.67	3.274		9	200.8	−33.6	N	23H-1-87	192.07	4.635		24	251.4	−54.1	N
16H-3-71	141.51	4.281	35	21	177.6	60.2	R	23H-2-139	194.09	0.586		*NR	235.4	−19.3	N
16H-3-142	142.22	6.765	60	26	159.0	68.8	R	23H-3-63	194.83	1.480		24	197.5	−17.6	N
16H-4-46	142.76	3.994	60	37	152.0	61.7	R	23H-3-137	195.57	1.695		18	200.5	−28.8	N
16H-4-86	143.16	2.161		32	161.3	47.3	R	23H-4-12	195.82	1.058		23	146.3	47.8	R
16H-5-12	143.92	2.977		35	14.0	49.0	R	23H-4-136	197.06	3.931		26	114.7	66.7	R
16H-5-87	144.67	0.871		*27	201.6	−34.0	N	23H-5-42	197.62	3.901		7	180.4	67.6	R
16H-6-16	145.49	1.033		38	176.8	−5.7	?	24H-1-13	198.33	2.268		29	126.5	73.5	R
16H-6-86	146.19	2.524		33	252.5	−73.7	N	24H-2-16	199.86	3.156	37.5	31	171.7	83.6	R
16H-7-13	146.96	2.602		24	250.2	−71.6	N	24H-2-88	200.58	2.283		10	173.6	55.7	R
16H-7-44	147.27	2.869	50	39	218.4	−59.5	N	24H-3-65	201.85	5.037		16	181.7	19.3	R
17H-1-71	148.21	3.125		17	160.8	−37.0	N	24H-3-120	202.40	4.323		7	187.7	−20.7	N
17H-1-141	148.91	6.272		12	180.0	−2.2	?	24H-4-13	202.83	5.477		22	178.8	−14.9	N
17H-2-14	149.14	4.544		15	143.0	6.5	?	24H-4-88	203.58	2.808		17	168.1	11.0	R
17H-2-89	149.89	1.835		13	93.9	21.4	R	25H-1-53	204.73	3.416		7	140.1	67.9	R
17H-3-56	151.06	7.213		19	117.5	−60.2	N	25H-1-133	205.53	3.777		19	166.0	−37.8	N
17H-3-126	151.76	7.799		8	180.9	−24.4	N	25H-2-67	206.37	2.243		20	185.9	55.5	R
17H-4-14	152.17	11.430		8	151.8	−64.2	N	25H-3-93	208.13	1.785		17	225.9	−42.1	N
17H-4-106	153.09	9.065		6	176.7	−29.9	N	25H-4-16	208.86	2.142		6	185.1	42.2	R
17H-5-6	153.59	7.293		9	135.4	−85.0	N	25H-5-16	210.36	2.567		18	179.2	7.3	?
17H-5-64	154.17	9.135		7	195.8	−35.9	N	25H-5-138	211.58	4.812	20	NR	190.8	−47.5	N
17H-6-88	155.91	7.347		23	174.9	65.0	R	25H-6-43	212.13	5.505		20	181.7	−49.1	N
17H-6-136	156.39	5.031		*33	102.9	83.8	R	25H-6-143	213.13	2.074		22	201.5	−20.1	N
18H-1-54	157.74	4.734		13	329.8	82.9	R								
18H-2-44	159.14	3.176		*5	253.4	53.2	R								
18H-2-142	160.12	6.114		7	244.5	43.0	R								
18H-3-43	160.63	7.598		7	234.3	57.1	R								
18H-3-141	161.61	8.382		14	160.3	60.0	R								
18H-4-13	161.83	2.722		16	174.1	59.4	R								
18H-5-106	164.26	4.780		*4	202.1	52.8	R								
18H-6-69	165.39	0.372	50	37	182.4	74.4	R								

along the 180° local azimuth (which is directly out of the core face), when we would expect randomly orientated core-mean declinations. The ~90° difference in the declination between the clusters of Spiess and ourselves is assumed to reflect a different choice of azimuthal origin. Furthermore, many of the specimens exhibit low to moderate inclinations (see also Figs 3c and d) when we would predict inclinations of 80° (with related scatter resulting from geomagnetic secular variation) for this site, assuming deposition at 70°S (based on the Cambridge Palaeomap Services Atlas 1993).

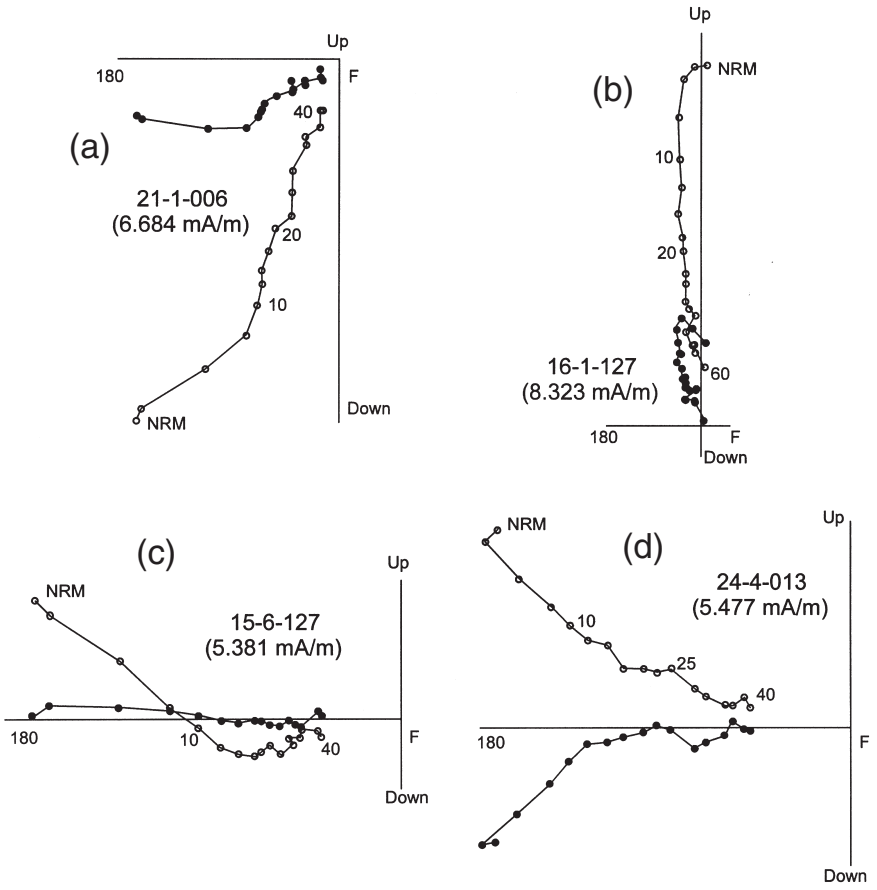

Figure 3. Zijderveld (1967) plots illustrating demagnetization behaviour typical of specimens from Hole 690B. Closed circles represent the remanence vector on the horizontal planes, F/180 being into/out of the split core face. Open circles represent the remanence vector on the F-180 orientated vertical plane. Numbers indicate the applied alternating demagnetization field in mT. Sample identifiers and the initial NRM intensity are shown.

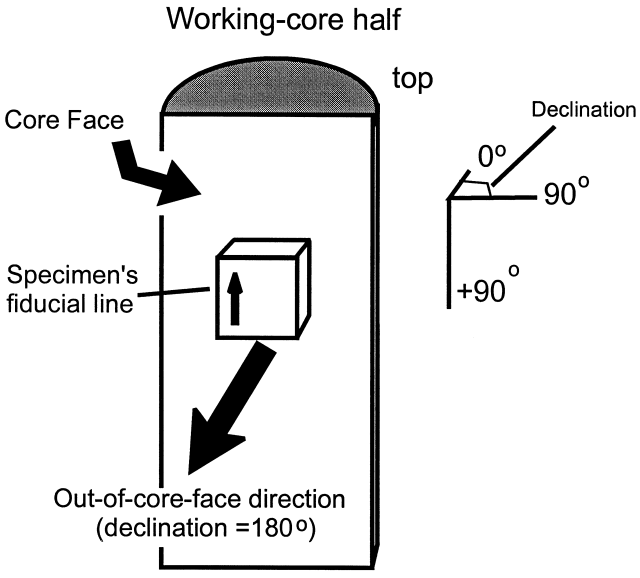

Figure 4. Reference frames used in discussing directional data.

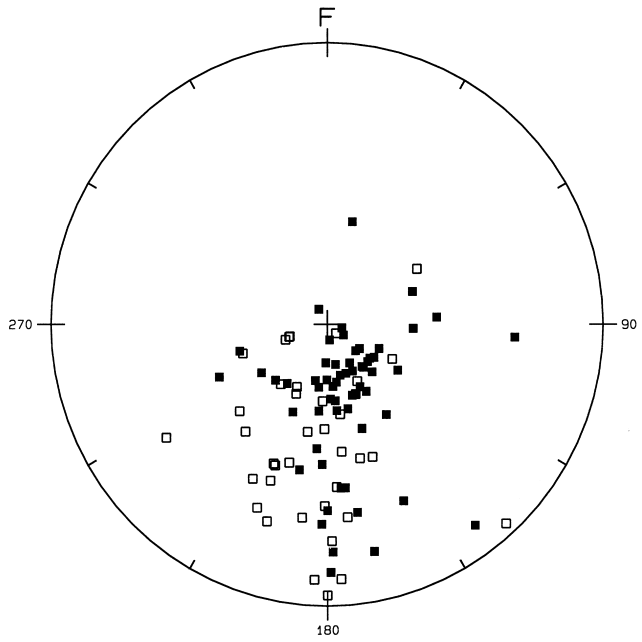

Figure 5. Stereographic plot showing ChRM directions for specimens examined in this study (from Sections 14H-5 to 25H-6). Open/closed squares represent ChRM directions pointing up/down, respectively. F is an arbitrary azimuth directed into the split core face.

The stratigraphic plot of ChRMs (Fig. 6) offers further insights into the spurious magnetizations recorded in Hole 690B. The declination plot indicates that the 180° clustering is a pervasive feature of the studied section; we do not see large

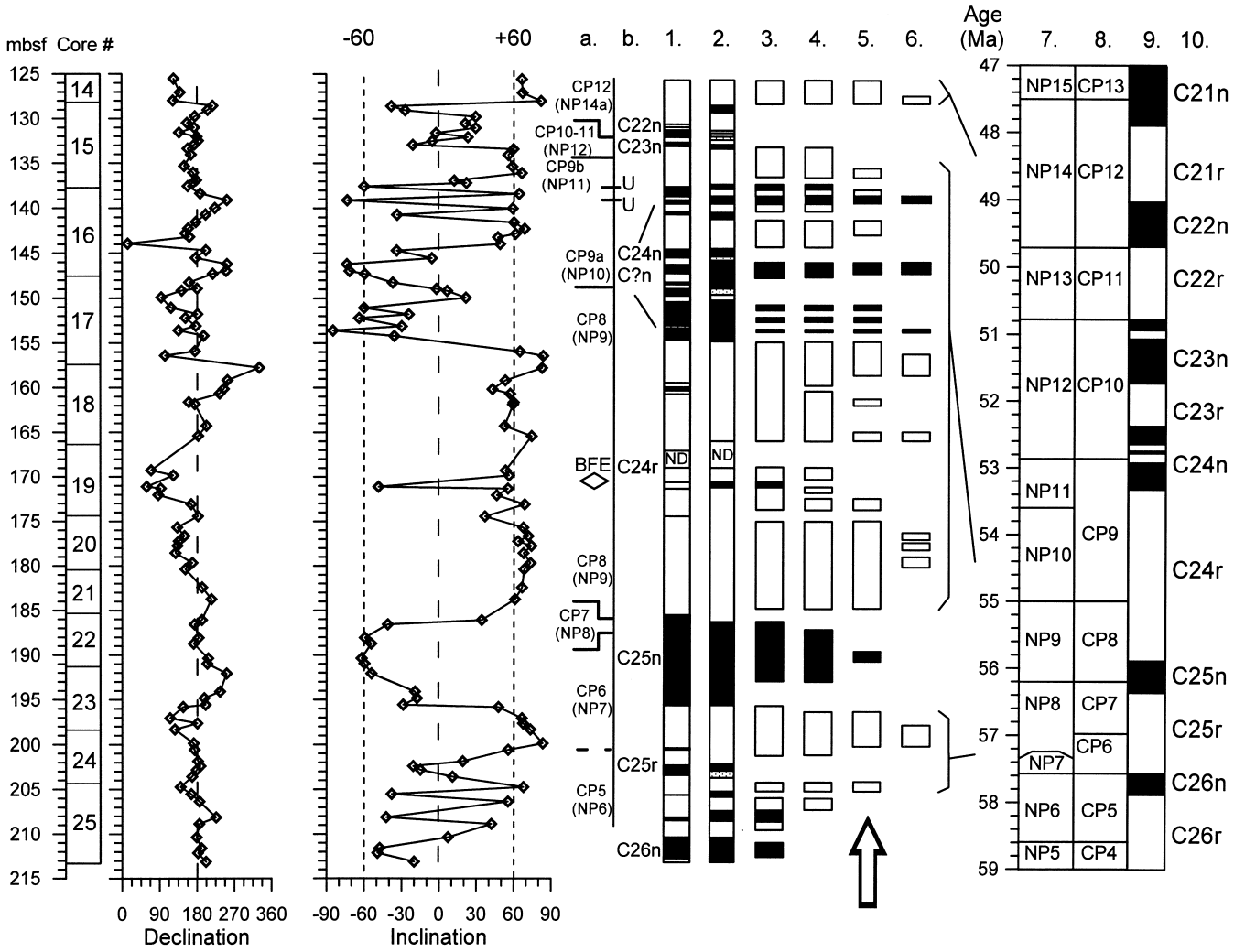

Figure 6. Hole 690B ChRM data and a filtered magnetostratigraphy for the upper Palaeocene–lower middle Eocene interval in Hole 690B. Zero declination is directed into the split face of the working core. Column (a): nannofossil zonation from Pospichal & Wise (1990) and Aubry *et al.* (1996). BFE: benthic foraminiferal extinction event; U: position of unconformable surfaces based on Aubry *et al.* (1996; p 358). Column (b): magnetic polarity assignments: (1) Spiess's (1990); (2) this study all ChRM data; (3) ditto, for absolute inclinations (Inc) $\geq 40.0^{\circ}$; (4) Inc $\geq 50.0^{\circ}$; (5) Inc $\geq 60.0^{\circ}$ and (6) Inc $\geq 70.0^{\circ}$. Black = normal polarity, white = reverse, shaded = indeterminate. Columns 7–10: magnetobiostratigraphic timescale information from Berggren *et al.* (1995). On the inclination plot, the $-60/+60$ tramlines highlight the specimens used to construct the magnetostratigraphy in Column 5 (the time-averaged axial dipole inclination during deposition would have been about 80° at Site 690).

within-core scatter, as we might expect at this high-latitude site, and random core-mean declinations. The inclination plot shows stratigraphic intervals where some values are similar to those predicted by the time-averaged geocentric axial dipole model, for example 176–184 mbsf, but others where they are noticeably low, for example 129–133 and 202–213 mbsf.

Based on the stratigraphic plots, additional observations pertinent to the Hole 690B magnetizations are as follows.

(1) Within each core there is no systematic pattern to ChRM directions with depth.

(2) There is no obvious link between the penetration of individual cores, which in its crudest form reflects the mechanical strength of the sediment across particular intervals, and ChRM directions.

(3) In most cases, trends in the pattern of ChRM directions appear to cross core boundaries without major jumps, suggesting that such behaviour is stratigraphically controlled; that is, physical and/or chemical properties of the sediments at specific levels.

(4) Alternate cores do not show the core-barrel remagnetization effect as demonstrated by D. Schneider and D. Vandamme (in Backman *et al.* 1988).

INTERPRETING THE HOLE 690B OVERPRINT

Several types of secondary magnetization have been reported from studies of soft to partially lithified piston-cored sediments (e.g. Barton & Bloemendal 1986; Bleil 1989; Tauxe *et al.* 1989; Roberts *et al.* 1996). In explaining the pervasive spurious component in the Hole 690B data, we consider that the critical observation is that the magnetization is out of the face. Thus, we suggest that one of the two following mechanisms is the most likely explanation for the 690B overprint.

(1) An inward-radial remagnetization as documented by D. Schneider and J.-P. Valet (in Curry *et al.* 1995), Fuller *et al.* (1997) and Fuller *et al.* (1998), who invoke cutting-shoe and/or core barrel fields as the sediment's remagnetizing agent.

(2) A core-split remagnetization (e.g. Witte & Kent 1988): the steep upward dipping field (about -63° according to Baldwin & Langel 1993) at the Hole 690B splitting site would have intersected the horizontally lain face of each halved core at a high angle.

The most appropriate method for distinguishing between these overprints is by analysing sister samples from the same stratigraphic level, with each offset a similar amount, say a cm or so, from the core's long axis. Sister specimens recording inward-radial magnetizations will have different declinations. Paired specimens recording core-split overprints will have ChRM declinations that are effectively identical. As regards Hole 690B, it is not possible to determine which of the two suggested mechanisms is responsible for the overprint, as paired sampling was not carried out.

ATTEMPT AT ERECTING A MAGNETOSTRATIGRAPHY FOR THE 690B SECTION

From the directional information shown in Fig. 6, it is clear that that the 690B section is not uniformly overprinted. Thus the key practical consideration is whether the overprint masks the primary signal completely and, if not, is it possible to erect a magnetostratigraphy for the hole. Fuller *et al.* (1998) suggested that it was possible to construct a magnetostratigraphy using data from the inward-radial remagnetized cores they analysed, 'because the latitude of the site gave a strong vertical component of magnetization from which polarity could usually be determined'. Witte & Kent (1988) were able to isolate the primary signal in many of the core-split overprinted specimens they examined, and position the Brunhes–Matuyama boundary in some cores. However, they found that separating the primary direction from the overprint often required AF demagnetization in excess of 70 mT.

To construct a magnetostratigraphy for the 690B section, we used as a filter the degree of apparent overprinting within each specimen as measured by the magnitude of the inclination (heavy overprint = shallow inclination). With the high-latitude Maud Rise cores, where the inclination of the time-averaged geomagnetic field during deposition would have been $\sim 80^\circ$ we would expect the inward-radial/core-split overprint to be at a high angle to the primary ChRM. Declinations would be directed towards 180°, and absolute inclinations would be lower than the predicted (80°) values.

The right-hand part of Fig. 6 shows how the ChRM data are used to construct several progressively filtered magnetostratigraphic columns. The various biostratigraphic data (mainly nannofossil datums proposed by Pospichal & Wise 1990, with later minor modifications by Aubry *et al.* 1996) and the positions of the δC^{13} excursion and benthic foraminiferal extinction event (BFE) are shown. Column 1 is the scheme proposed by Spiess (1990, Appendix B). Column 2 is the magnetic polarity assignments resulting from the ChRM inclinations obtained in the present study. The new scheme clearly matches the previously obtained record, the minor differences reflecting the higher resolution afforded by Spiess's 25 cm sampling interval. Columns 3 to 6 show the magnetic polarity assignments using specimens with absolute inclinations of $\geq 40.0^\circ$, $\geq 50.0^\circ$, $\geq 60.0^\circ$ and $\geq 70.0^\circ$. The first filtered step (inclination $\geq 40^\circ$, Column 3) eliminates ChRM data from 33 specimens, and most of these are the 'noisy' normal-polarity samples in the intervals 128–142 and 201–212 mbsf. The $\geq 50.0^\circ$, $\geq 60.0^\circ$ and $\geq 70^\circ$ step schemes are based on 54, 35 and 13 specimens, respectively.

ATTEMPTED CORRELATION WITH THE GPTS

If the filtering process is a valid way of eliminating specimens with heavy overprints, it should then be possible to correlate the resultant magnetozones with the scheme of Berggren *et al.* (1995). A filtering level of absolute inclinations $\geq 60^\circ$ (Column 5) was chosen because there is a wide angular separation defining the two polarity states and a reasonable number of specimens on which to base the magnetostratigraphy.

Almost all of the specimens from the lower third of the section are eliminated. These include a block of normal-polarity samples at ~ 212 mbsf, which Spiess correlated with Chron C26n. Five reverse-polarity specimens that straddle the NP6/7 biozone boundary are possible records of Chron C25n. Previously, Chron C25n was identified in the section from about 195.8 up to 185.5 mbsf. Superficially that correlation was sensible since the top of the magnetozone as defined by Spiess, and in the unfiltered section generated by this study, lies just below the CP7/CP8 (= NP8/NP9) boundary. However, such a correlation raises two issues. The first is that the lowest occurrence of *Discoaster multiradiatus* (used to define the NP8/NP9 boundary in Hole 690B and globally) in Spiess's (1990) section must correspond to a minor unconformity, since the end of Chron C25n is positioned within the early part of the NP9 biochron. A more critical concern is that the base of Spiess's C25n magnetozone extends well down into NP7, making it about 1 Myr older than in the timescale of Berggren *et al.* (1995). The filtering appears to have resolved this conundrum. The single normal-polarity specimen at 190.38 mbsf (see Table 1) is unlikely to be a record of Chron C25n as it is positioned in the NP7 biozone.

The section between 183.75 and 136.0 mbsf carries a dominantly reverse polarity. The work of Pospichal & Wise (1990) and Aubry *et al.* (1996) indicates that this interval spans nannofossil zones NP9 to lower NP11. Therefore, the linkage of the reverse-polarity interval with Chron C24r is the most appropriate correlation, as proposed earlier by Aubry *et al.* (1996). 10 of the 15 specimens that make up the unfiltered ~ 10 m thick normal-polarity magnetozone centred on 150 mbsf are eliminated from the succession (they are in fact removed at the lowest filtering level). Of the five normal-polarity specimens that remain, only two are from adjacent levels, and what is left of the magnetozone must be regarded with some suspicion. It is not a record of C24n, which is what Spiess proposed; it sits at a level linked biostratigraphically to mid Chron C24r. The concerns Aubry *et al.* (1996) had regarding the validity of this magnetozone as a record of Chron C24n were justified.

Three reverse-polarity samples are present at the very top of the studied section. As these sediments are assigned to nannofossil zone CP12 (NP14a), linkage with Chron C21r is the most appropriate correlation.

SUMMARY

To extract a magnetostratigraphy from the Hole 690B section, we have applied a filtering scheme to eliminate critically overprinted levels from the record. The most important features of this new scheme are as follows.

(1) The previously questionable Chron C25n magnetozone is eliminated.

(2) The Chron C24r interval is considerably cleaner.

(3) Many of the specimens used previously to define a normal-polarity magnetozone in levels that correlate biostratigraphically with mid Chron C24r carry strong overprints. This magnetozone is not a record of Chron C24n as was thought previously.

The Palaeocene/Eocene boundary events are known to sit within Chron C24r, but we are unable to fix either the upper or lower boundary of this magnetochon in Hole 690B. Thus age-calibrating of these events in Hole 690B must be based on the biostratigraphy alone.

CONCLUSIONS

The Palaeocene/Eocene boundary interval in Hole 690B carries a secondary magnetization in the form of an inward-radial or core-split overprint. Attempts to generate a filtered magnetostratigraphy for the upper Palaeocene to middle Eocene section in Hole 690B have met with some success. In particular, critical magneto–biozone mismatches identified previously appear to be the result of the overprinting. With the new scheme it is not possible to position the reversal boundaries marking the start and end of Chron C24r. Thus we recommend that dating key levels within the Hole 690B section, that is the O and C isotope excursions and late Palaeocene benthic foraminiferal extinction, be based exclusively upon the nannofossil biostratigraphy.

The present study has involved a re-examination of just the upper Palaeocene to lower middle Eocene section in Hole 690B. A cursory glance of the data from other levels within this hole (Spiess 1990, Appendix B) shows the same pervasive declination cluster that prompted this reinvestigation. Before drawing on those magnetostratigraphic data to provide age control, for example Ramsay & Baldauf's (1999) Southern Ocean biochronology synthesis, palaeomagnetic reinvestigations should be considered to establish whether the cores carry secondary overprints that completely mask the original polarity of specific levels.

ACKNOWLEDGMENTS

This paper is dedicated to the memory of Mr Syed Asghar Ali. JRA is grateful to John Malpas, Head of the Earth Science Department at the University of Hong Kong, for the support that he has given to this study, and to Andy Roberts, Southampton Oceanography Centre, for allowing him to run material in his laboratory and for discussions on spurious magnetizations. Sarah Draper-Ali, Paula Weiss and Drew Patrick helped with sampling. Periodic discussions with Mark Cryer on soft sediment deformation are acknowledged. Correspondence with David Schneider regarding spurious remanences encountered on ODP Legs 115, 138 and 154 have also proved useful. We thank Charlie Barton, Gary Acton and Yves Gallet for critical reviews. This is LDEO contribution no. 5888.

REFERENCES

Ali, J.R. & Hailwood, E.A., 1998. Resolving possible problems associated with the magnetostratigraphy of the Paleocene/Eocene boundary in Holes 549, 550 (Goban Spur) and 690B (Maud Rise), *Strata,* **9,** 16–20.

Aubry, M.-P., Berggren, W.A., Stott, L. & Sinha, A., 1996. The upper Paleocene-lower Eocene stratigraphic record and the Paleocene–Eocene boundary carbon isotope excursion: implications for geochronology, in *Correlation of the Early Paleogene in NW Europe,* eds Knox, R.W.O'B., Corfield, R.M. & Dunay, R.E., *Geol. Soc. Lond. Spec. Publ.,* **101,** 353–380.

Backman, J. *et al*., 1988. *Proc. ODP, Init. Repts,* **115,** 1085.

Baldwin, R.T. & Langel, R., 1993. Tables and maps of the DGRF 1985 and IGRF 1990, *IAGA Bull.,* **54,** 117.

Barton, C.E., Bloemendal, J., 1986. Paleomagnetism of sediments collected during Leg 90, Southwest Pacific, *Init. Repts DSDP,* **90,** 1273–1316.

Berggren, W.A., Kent, D.V., Swisher, C.C. III & Aubry, M.-P., 1995. A revised Cenozoic geochronology and chronostratigraphy, in *Geochronology, Time Scales and Stratigraphic Correlation: Framework for an Historical Geology,* eds Berggren, W.A., Kent, D.V., Aubry, M.-P. & Hardenbol, J., *Soc. Econ. Paleont. Min. Spec. Publ.,* **54,** 129–212.

Bleil, U., 1989. Magnetostratigraphy of Neogene and Quaternary sediment series from the Norwegian Sea, *Proc. ODP Sci. Res.,* **104,** 829–901.

Cambridge Paleomap Services., 1993. *Atlas,* Version 3.3, Cambridge Paleomap Services, PO Box 246, Cambridge.

Curry, W.B. *et al*., 1995. *Proc. ODP, Init. Repts.,* **154,** 1111.

Fisher, R.A., 1953. Dispersion on a sphere, *Proc. R. Soc. Lond., A,* **217,** 295–305.

Fuller, M., Herro-Bervera, E., Frost, G., Herr, B., Hastedt, M. & Garrett, E., 1997. Magnetic contamination acquired during APC coring, *EOS, Trans. Am. geophys. Un.,* **78,** F186.

Fuller, M., Hastedt, M., Herr, B., 1998. Coring induced magnetization of recovered ODP sediment, *Proc. ODP. Sci. Res.,* **157,** 47–56.

Hailwood, E.A., Clement, B.M., 1991. Magnetostratigraphy of Sites 703 and 704, Meteor Rise, southeastern South Atlantic, *Proc. ODP Sci. Res.,* **114,** 367–385.

Hailwood, E.A., Stumpp, C. & Zukin, J., 1989. Soft sediment sampling errors in palaeomagnetic and magnetic fabric data, *Bull. Int. Assoc. Geomagn. Aeron.,* **53,** 199 (Abstract).

Kennett, J.P. & Stott, L.D., 1991. Abrupt deep-sea warming, paleoceanographic changes and benthic extinctions at the end of the Paleocene, *Nature,* **353,** 225–229.

Kirschvink, J.L., 1980. The least squares line and plane analysis of paleomagnetic data, *Geophys. J. R. astr. Soc.,* **62,** 699–718.

Koch, P.L., Zachos, J.C. & Dettman, D.L., 1995. Stable isotope stratigraphy and paleoclimatology of the Paleogene Bighorn basin (Wyoming, USA), *Palaeogeog., Palaeoclimat. Palaeoecol.,* **115,** 61–89.

Lovlie, R., Markussen, B., Sejrup, H.P. & Thiede, J., 1986. Magnetostratigraphy in three Arctic Ocean sediment cores; arguments for geomagnetic excursions within oxygen-isotope stage 2–3, *Phys. Earth planet. Inter.,* **43,** 173–184.

Pospichal, J.J. & Wise, S.W., 1990. Paleocene to middle Eocene calcareous nannofossils of ODP Sites 689 and 690, Maud Rise, Weddell Sea, *Proc. ODP Sci. Res.,* **113,** 613–638.

Ramsay, A.T.S. & Baldauf, J.G., 1999. A reassessment of the Southern Ocean Biochronology, *Geol. Soc. Lond. Mem.,* **18,** 122.

Roberts, A.P., Stoner, J.S., Richter, C., 1996. Coring-induced magnetic overprints and limitations of the long-core paleomagnetic measurement technique: some observations from Leg 160, eastern Mediterranean Sea, *Proc. ODP, Init. Repts,* **160,** 497–505.

Spiess, V., 1990. Cenozoic magnetostratigraphy of Leg 113 drill sites, Maud Rise, Weddell Sea, Antarctica, *Proc. ODP Sci. Res.,* **113,** 261–315.

Stott, L.D. & Kennett, J.P., 1990. Antarctic Paleogene Planktonic foraminiferal biostratigraphy, *Proc. ODP Sci. Res.,* **113,** 549–570.

Stott, L.D., Kennett, J.P., Shackleton, N.J. & Corfield, R.H., 1990. The evolution of Antarctic surface waters during the Paleogene: inferences from the stable isotopic composition of planktonic foraminifera, *Proc. ODP Sci. Res.,* **113,** 849–864.

Stott, L.D., Sinha, A., Thiry, M., Aubry, M.-P. & Berggren, W.A., 1996. Global $\delta^{13}C$ changes across the Paleocene/Eocene boundary: criteria for terrestrial-marine correlations, in *Correlation of the Early Paleogene in NW Europe,* eds Knox, R.W.O'B., Corfield, R.M. & Dunay, R.E., *Geol. Soc. Lond. Spec. Publ.,* **101,** 381–399.

Tauxe, L., Valet, J.-P., Bloemendal. J., 1989. Magnetostratigraphy of Leg 108 advanced piston cores, *Proc. ODP Sci. Res.*, **108,** 429–439.

Thomas, E., 1990. Late Cretaceous through Neogene deep sea-foraminifers, Maud Rise, Weddell Sea, Antarctica, *Proc. ODP Sci. Res.,* **113,** 571–594.

Thomas, E. & Shackleton, N.J., 1996. The Paleocene-Eocene benthic foraminiferal extinction and stable isotope anomalies, in *Correlation of the Early Paleogene in NW Europe,* eds Knox, R.W.O'B., Corfield, R.M. & Dunay, R.E., *Geol. Soc. Lond. Spec. Publ.,* **101,** 401–441.

Witte, W.K. & Kent, D.V., 1988. Revised magnetostratigraphies confirm low sedimentation rates in Arctic Ocean cores, *Quat. Res.,* **29,** 43–53.

Zijderveld, J.D.A., 1967. AC demagnetization of rocks: analysis of results, in *Methods in Palaeomagnetism,* pp. 254–286, eds Collinson, D.W., Creer, K.M. & Runcorn, S.K., Elsevier, New York.

Zachos, J., Rea, D., Seto, K., Nomura, R. & Niitsuma, N., 1992. Paleogene and early Neogene deep water paleoceanography of the Indian ocean as determined from benthic foraminifer stable carbon and oxygen isotope records, *Am. geophys. Un., Geophys. Monogr.,* **70,** 351–386.

Zachos, J., Stott, L.D. & Lohmann, K.C., 1994. Evolution of early Cenozoic temperatures, *Paleoceanography,* **9,** 353–387.